Penerbit Akademia Baru

Journal of Advanced Research in Micro and Nano Engineering

Journal homepage: https://akademiabaru.com/submit/index.php/armne

ISSN: 2756-8210

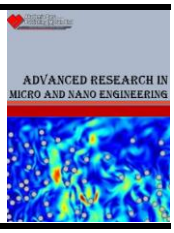

Activity of Viscoelastic Nanofluid Film Sprayed on a Stretching Cylinder with Arrhenius Activation Energy and Entropy Generation

Auwalu Hamisu Usman[1,2], Sadiya Ali Rano[2], Usa Wannasingha Humphries[1,*], Poom Kumam[1]

[1] Department of Mathematics, Faculty of Science, King Mongkut's University of Technology Thonburi (KMUTT), 126 Pracha-Uthit Road, Bang Mod, Thung Khru, Bangkok 10140, Thailand

[2] Department of Mathematics, Faculty of Science, Bayero University Kano, Nigeria

ABSTRACT

The performance of viscoelastic nano-liquid film sprayed over a stretched cylinder is investigated. It also explores the effects of activation energy and the assessment of entropy on heat and mass flow. Similarity transformations have been used to make the governing equations dimensionless and successively resolved by a strong analytical technique homotopy analysis method (HAM). The velocity decreases with the magnetic field strength and the viscoelastic nanofluid parameters. The temperature increases with the Brownian motion parameter while it decreases with the increasing of Prandtl number, film thickness parameter and thermophoresis parameter. The concentration of nanoparticles is enhanced by the higher Reynolds number and the activation energy parameter. The film size causes increased with the spray rate in a nonlinear way. The two-dimensional case is recovered in the Reynolds number and film thickness limit values. A close agreement is reached by comparing the current with published results. The results obtained, perhaps in ideal circumstances, would be useful for the analysis and design of applications for coating.

Keywords:
Viscoelastic nanofluid, Film spray, Arrhenius activation energy, Binary chemical reaction, HAM, Entropy generation

1. Introduction

Progress in non-Newtonian liquids is of great importance for projects and emerging developments. Magnetic hydrodynamics applied to electrically conductive fluids primarily concerned with the results that can be derived from the connection between any external magnetic field current and fluid motion. Albano *et al*. [1] investigate and reported that metallurgy (form control, homogenization, sample levitation material), molten steel flow, planetary science and astrophysics, fusion reactors are some of non-Newtonian main applications. Due to its exceptional behaviour, the viscoelastic fluid model is essential for the type of fluid. Han *et al*. [2] investigated on the viscoelastic fluid coupled with the Cattaneo–Christov heat flux model. Mrokowska and Krztoń-Maziopa [3] reported on viscoelastic and shear-thinning effects on disk and sphere of the aqueous exopolymer

* *Corresponding author.*
E-mail address: ahu3802@gmail.com

solution. Li *et al*. [4] studied the MHD viscoelastic flow and heat transfer through a vertical stretching sheet with heat flow effects from Cattaneo-Christov. More detail on non-Newtonian fluids can be seen in the references [5-8].

Liquid cooling is improved by nano-sized particles with a diameter of between 1 and 100 nm. These nanoparticles are mixed with the base fluid that improves the cooling process due to its higher coefficient of heat transfer compared to conventional liquids. This mixture is called a nanofluid. Choi and Bestman [9] introduced the concept of nanofluid at Argonne National Laboratory, USA. Nanotechnology is one of the most interesting field nowadays. It is often a special type of fluid with higher thermal conductivity than conventional host fluids. Buongiorno [10] Reported and also implemented a second phase nanofluid model in the awake of these models. Ellahi *et al*. [11] studied the heated couple stress bi-phase fluid with spherical particles of metal Hafnium. In the paper the flow bounded by two parallel plates is caused by solely the influence of pressure gradient in an axial direction.

Thin film flow is considered to be an essential subject of study. Thin film fluids are used for the production of different heat exchangers and chemical tools, but these applications require a total comprehension of the motion procedure. Thin film fluid applications included wire and fiber coating, polymer preparation, etc. This motion is attached to the manufacture of different types of sheets, if either metal or plastic. Some researchers have considered working on this type of flow in recent years. Ellahi *et al*. [12] investigated on the thin film coating on multi-fluid flow of a rotating disk suspended with nano-size silver and gold particles. Further research work has been carried out in the references [13-15].

One of the most significant indicators is that the species does not normally respond to chemical reactions with Arrhenius activation energy. The term activation energy was originally investigated by Arrhenius [16]. However, the minimum energy needed for the process of molecules or atoms of chemical reactions is classified as activation energy. Perhaps for the first time, Bestman [17] identified a primary model consisting of a boundary layer of fluid flow problems due to binary chemical reactions with Arrhenius activation energy. The emphasis here is on the flow of a binary chemical reacting fluid with Arrhenius activating energy and convective boundary conditions. One of the objectives of this research article is to evaluate the effect of activation energy on fluid flow and binary chemical reactions. Further research work has been carried out in the references [18-22].

It has been noted that due to the stretching of the cylinder, proper attention is paid to the stretching of the flow of the cylinder. Wang [23] first to study the steady-state incompressible viscous fluid across the growing hollow cylinder. Bachok and Ishak [24] examined and reported the numerical flow and thermal transfer solution for the stretching cylinder. Chuhan *et al*. [25] investigated the effects of magnetohydrodynamics and thermal radiation on the movement of fluid past a porous stretching cylinder. Further research work has been carried out in the references [26-27].

Literature has a number of interesting studies on stretching cylinders that are accompanied by this study. Until now, no investigation into the current problem has been carried out to the best of knowledge. This article analyses the steady two-dimensional, incompressible radiative flow of the viscoelastic axisymmetric sprayed thin film nanofluid past the stretching cylinder. The fluid flow problem is controlled by partial differential equations and is transformed into ordinary ones by appropriate similarity transformations. Initially, Liao presented HAM in 1992 [28-30]. The solution of this method is fast convergent. Due to its rapid convergence, various researchers [31-32] have used HAM to solve their fluid flow problems. The results obtained for the effects of all related parameters on all profiles are graphically presented.

2. Mathematical Formulation

The steady, two-dimensional, and incompressible flow of viscoelastic and axisymmetric sprayed thin film nanofluid is considered past a stretching cylinder at $r=0$. The flow is in the domain $r>0$. The $z-axis$ is taken along the axis of cylinder and $r-axis$ is measured along the radial direction. The effects of the magnetic field are used in the direction of $r-axis$. Assuming induced magnetic field effects to be negligible. A radial axisymmetric spray with velocity V condenses as a film and is drawn along the cylinder's outer surface, see Figure 1. Let T and C represent the temperature and concentration of nanoparticles respectively. The concentrations of nanoparticles near the surface is represented by C_w. In addition, beyond the surface, C_b symbolizes the concentration of nanoparticles.

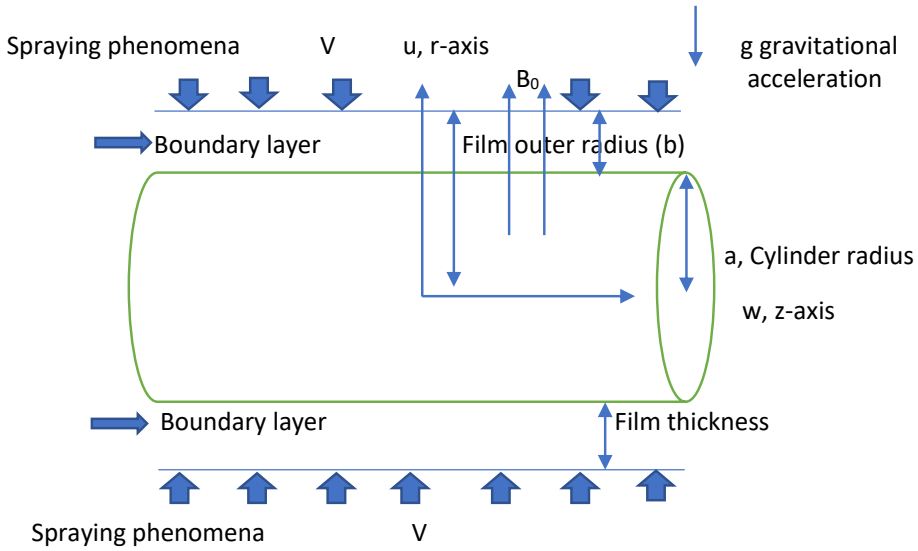

Fig. 1. Geometry of the Problem

The modelled fluid flow equations are [13,25-26]

$$\frac{\partial u}{\partial r}+\frac{u}{r}+\frac{\partial w}{\partial z}=0, \tag{1}$$

$$u\frac{\partial w}{\partial r}+w\frac{\partial w}{\partial z}=\nu\left[\frac{\partial^2 w}{\partial r^2}+\frac{1}{r}\frac{\partial w}{\partial r}\right]-\sigma B_o^2 w+\frac{k_o}{\rho_f}\left[\begin{array}{l} w\frac{\partial^3 w}{\partial r^3}+w\frac{\partial^3 w}{\partial z\partial r^2}-\frac{\partial w}{\partial r}\frac{\partial^2 u}{\partial r^2}+\frac{\partial w}{\partial z}\frac{\partial^2 w}{\partial r^2}+ \\ \frac{1}{r}\left(u\frac{\partial^2 w}{\partial r^2}+w\frac{\partial^2 w}{\partial z\partial r}-\frac{\partial u}{\partial r}\frac{\partial w}{\partial r}+\frac{\partial w}{\partial z}\frac{\partial w}{\partial r}\right) \end{array}\right]+ \tag{2}$$

$$\frac{1}{\rho_f}\left[(1-C_b)\rho_f\beta^*(T-T_b)-(\rho_p-\rho_f)(C-C_b)\right]g$$

$$u\frac{\partial T}{\partial r}+w\frac{\partial T}{\partial z}=\alpha_1\left[\frac{\partial^2 T}{\partial r^2}+\frac{1}{r}\frac{\partial T}{\partial r}\right]+\tau\left[D_B\frac{\partial C}{\partial r}\frac{\partial T}{\partial r}+\frac{D_T}{T_b}\left(\frac{\partial T}{\partial r}\right)^2\right]-\frac{1}{(\rho c)_f}\frac{\partial (rq_r)}{\partial r} \tag{3}$$

$$u\frac{\partial C}{\partial r}+w\frac{\partial C}{\partial z}=D_B\frac{1}{r}\frac{\partial}{\partial r}\left(r\frac{\partial C}{\partial r}\right)+\frac{D_T}{T_b}\frac{1}{r}\frac{\partial}{\partial r}\left(r\frac{\partial T}{\partial r}\right)-k_r^2\left(C-C_b\right)\left(\frac{T}{T_b}\right)^n\exp\left[\frac{-E_a}{kT}\right] \quad (4)$$

With boundary conditions

$$w(z,r)=W_w(z),\ \ u(z,r)=U_w(z),\ \ T(z,r)=T_w(z),\mathrm{C}(z,r)=C_w(z)\ \text{at}\ r=a, \quad (5)$$

$$\frac{\partial w}{\partial r}=0,\frac{\partial \delta}{\partial r}=0,\frac{\partial C}{\partial r}=0,\frac{\partial T}{\partial r}=0,\ u=\frac{\partial \delta}{\partial z}\ \text{at}\ r=b\,, \quad (6)$$

where δ is the film size, B_o is the magnetic field strength, σ is the electrical conductivity, k_0 is the relaxation time coefficients, g is the gravity acceleration, ρ_p stands for the liquid density, v_f is the kinematic viscosity, u and w are velocity components, the nanoparticles volume is C, the fluid temperature is T, ρ_f is the density of base fluid, α_1 is the thermal diffusivity, D_B is the Brownian motion, D_T is the thermophoretic diffusion coefficient, and the heat capacity ratio is τ.

According to the Rosseland approximation the thermally developed flow can be expressed as a modification [8] with σ^{**} is represented as Stefan-Boltzmann constant and k^{**} as the mean absorption coefficient.

$$q_r=-\frac{16\sigma^{**}T_b^3}{3k^{**}}\frac{\partial T}{\partial r}\,, \quad (7)$$

Introducing the transformation for non-dimensionless functions f,θ,ϕ and similarity variable ζ [13] as

$$\zeta=\left(\frac{r}{a}\right)^2,u=-ca\frac{f(\zeta)}{\sqrt{\zeta}},w=2czf'(\zeta),T(z)=T_b-T_{ref}\left[\frac{cz^2}{v_{\eta f}}\right]\theta(\zeta),\mathrm{C}(z)=C_b-C_{ref}\left[\frac{cz^2}{v_{\eta f}}\right]\phi(\zeta). \quad (8)$$

At the outer radius b of the film thickness with β_1 as the nondimensional film thickness parameter.

$$\zeta=\left(\frac{b}{a}\right)^2=\beta_1, \quad (9)$$

Eq. (1) is satisfied through Eq. (8-9) whereas Eq. (2)-(6) have the following form

$$\frac{1}{\mathrm{Re}}(2f''+2\zeta f''')-Mf'+ff''-f'^2+\lambda_1\left(4ff'f''+\frac{1}{\zeta}f^2f''-2f^2f'''-2Mff''\right)+$$
$$2\lambda_2\left[2\zeta f'f'''+\frac{2}{\zeta}ff''-ff'''+2\zeta f''^2-2ff'f'''-\frac{2}{\zeta}ff'f''\right]-Gr\theta+Gm\phi=0\,, \quad (10)$$

$$(2+Rd)(\theta'+\zeta\theta'')-Nb\phi'\theta'-Nt\theta'^2+Pr(f\theta'-2f'\theta)=0\,, \quad (11)$$

$$Sc(\phi'+\zeta\phi'')+f\phi'-2f'\phi+\tfrac{Nt}{Nb}(\theta'+\zeta\theta'')-\gamma_1\left(\gamma_2-\theta_w\theta\right)^2e^{-\left[\frac{E}{(\gamma_2-\theta_w\theta)}\right]}=0\,, \quad (12)$$

with boundary conditions given by

$$\begin{aligned} f = f' = \theta = \phi = 1 \ \ at \ \varsigma = 1 \\ f'' = \theta' = \phi' = 0 \ \ at \ \varsigma = \beta_1 \end{aligned}, \tag{13}$$

where Gr is the thermal Grashof number, Re is Reynolds number, M is the parameter of the magnetic field, Pr is the Prandtl number, Gm is the solutal Grashof number, Nt is the parameter of thermophoresis, Nb is the parameter of Brownian motion, Sc is the Schmidt number, Rd is the radiation parameter, λ_1 is the viscoelastic parameter, γ_1 is chemical reaction rate constant, γ_2 is the temperature ratio, θ_w is dimensionless wall temperature, E is the activation energy parameter, are defined as:

$$\begin{aligned} &\mathrm{Re} = \frac{ca^2}{\nu_f}, M = \frac{\sigma B_0^2}{2c\rho_f}, \lambda_1 = \frac{k_0 c}{\rho_f}, Gr = \frac{g\beta^*(1-C_b)(T_w - T_b)}{4c^2 a}, Gm = \frac{g(\rho_p - \rho_f)(C_w - C_b)}{4c^2 \rho_f a}, Rd = \frac{32\sigma^{**}T_\infty^3}{3(\rho c)_f k^{**}\alpha_1}, \\ &Nb = \frac{\tau D_B (C_w - C_b)}{\alpha_1}, \ Nt = \frac{\tau D_T (T_w - T_b)}{\alpha_1}, \ Sc = \frac{2D_B}{ca^2}, \ \ \gamma_1 = \frac{k_r^2}{2c}, \ \gamma_2 = \frac{T_w}{T_b}, \theta_w = \frac{T_w - T_b}{T_b}, \ \ E_1 = \frac{E_a}{kT_b}, \mathrm{Pr} = \frac{ca^2}{\alpha_1} \end{aligned}. \tag{14}$$

The shear stress on the surface of the outer film is zero i.e. $f''(\beta_1) = 0$. And the shear stress on the cylinder is $\tau = \dfrac{\rho_f \nu_f 4czf''(1)}{a} = \dfrac{4cz\mu_f f''(1)}{a}$.

The deposition velocity V in terms of film thickness β_1, Mass flux m_1 (interesting quantity which in connection with the deposition per axial length) and normalized mass flux m_2 are given respectively

$$ca\frac{f(\beta_1)}{\sqrt{\beta_1}} = V, m_1 = 2\pi bV \ \text{ and } \ m_2 = \frac{m_1}{2\pi a^2 c} = \frac{m_1}{4\pi \nu_f \,\mathrm{Re}} = f(\beta_1). \tag{15}$$

3. Physical Quantities

The physical quantities of interests such as skin friction C_f, Nusselt number Nu and Sherwood number Sh,
are given as following.

$$C_f = \frac{2\tau_{rz}}{\rho_f (W_w)^2}\Big|_{r=a} \text{ where } \tau_{rz} = \mu_f \left(\frac{\partial w}{\partial r}\right)_{r=a} \text{ therefore, } C_f = \frac{2}{\mathrm{Re}_z^{\frac{1}{2}}} f''(1). \tag{16}$$

$$Nu = \frac{aq_h}{k(T_w - T_b)}\Big|_{r=a} \text{ where } q_h = -k\frac{\partial T}{\partial r}\Big|_{r=a} \text{ therefore, } Nu = -2\theta'(1). \tag{17}$$

$$Sh = \frac{aq_m}{D_B(C_w - C_b)}\Big|_{r=a} \text{ where } q_m = -D_B\frac{\partial C}{\partial r}\Big|_{r=a} \text{ therefore, } Sh = -2\phi'(1). \tag{18}$$

4. Analysis of entropy generation

For the bio-nanofluid system, the irreversibility formulation with R denotes the ideal gas constant and D represents the diffusivity is

$$E'''_{gen}=\frac{\alpha_1}{T_b^2}\left[1+\frac{16T_1^3\sigma^*}{K(T)k^*}\right]\left(\frac{\partial T}{\partial r}\right)^2+\frac{\mu}{T_2}\left(\frac{\partial w}{\partial z}\right)^2+\frac{RD}{C_b}\left(\frac{\partial C}{\partial z}\right)^2+\frac{RD}{T_b}\left(\frac{\partial T}{\partial r}\frac{\partial C}{\partial r}+\frac{\partial C}{\partial z}\frac{\partial T}{\partial z}\right)+\sigma_{nf}B_o^2w^2, \quad (19)$$

In equation (19), the first term represents the irreversibility due to heat transfer, the second term is entropy generation due to viscous dissipation and third to six terms are irreversibilities due to diffusion effect. The seventh term stands for the entropy generation due to magnetic field. The characteristic entropy generation rate is

$$E_0'''=\frac{\alpha_1\left(T_a-T_b\right)^2}{T_b^2} \quad (20)$$

Notice that irreversibility $N_G\left(\varsigma\right)$ in scaled form is $N_G(\varsigma)=\frac{E'''_{gen}}{E_0'''}$ (21)

Using Eqn. (8), dimensional equation (19) converted into the following dimensionless form

$$N_G(\varsigma)=\frac{4}{a^2}\left(1+\frac{4}{3}Rd\right)\theta'^2+\frac{Br}{\theta_w^2}f''^2+B_1\left[\left(\frac{\phi_w}{\theta_w}\right)^2\phi^2+a^2\frac{\phi_w}{\theta_w}\phi'\theta'+\frac{\phi_w}{\theta_w}\phi\theta\right]+Mf'^2, \quad (22)$$

where N_G represents the entropy generation rate, $Br=\frac{4c^2\mu}{\alpha_1(T_w-T_b)}, B_1=\frac{4RDC_b}{\alpha_1}, M=\frac{4c^2a^2\sigma_{nf}B_0^2}{\alpha_1}$ are respectively the Brinkman number, diffusivity constant parameter due to nanoparticle concentration and magnetic field parameter. $\theta_w=\frac{\left(T_a-T_b\right)}{T_b}$, $\phi_w=\frac{\left(C_a-C_b\right)}{C_b}$, are respectively the dimensionless heat and nanoparticle concentration variables.

5. Solution by the homotopy analysis method (HAM)

Taking the initial guesses and the linear operators as

$$f_o(\zeta)=(1-e^{-\zeta}),\theta_o=e^{-\zeta},\phi_o=e^{-\zeta},\chi_o=e^{-\zeta},\ L_f=f'''-f',\quad L_\theta=\theta''-\theta,\quad L_\phi=\phi''-\phi, \quad (23)$$

satisfying the given properties below

$$L_f\left[C_1+C_2e^{\zeta}+C_3e^{-\zeta}\right]=0,\ L_\theta\left[C_4e^{\zeta}+C_5e^{-\zeta}\right]=0,\ L_\phi\left[C_6e^{\zeta}+C_7e^{-\zeta}\right]=0, \quad (24)$$

where $\{C_i\}_{i=1}^7$, are the arbitrary constants.

To complete the solution, we used Eq. (10) to (12) to find the zero and mth order in terms of the embedding parameter. Finally, Mathematica Software is used to find the final result and also to plot all the graphs.

6. Results and Discussion

A viscoelastic nanoliquid coolant and shielding paint or film sprays on a stretching cylinder. The normalized spray rate m_2 which is functionally correlated with the film size is shown in Figure 2(a). The film size naturally increases with the spray rate at once, but this does not happen linearly. The

outer surface of the film may be affected if the spray is not uniform. It is interesting that spray rate increases the thickness of the film in a non-linear form. Due to spray, the viscoelastic nanoliquid film is deposited on the stretching cylinder which can be used to cool the extruded material to promote solidification either by a water bath or spraying with a coolant. Spraying also provides better cooling since it creates thinner boundary layer.

It is observed from Figure 2(b) that the velocity profile is a decreasing function of the magnetic field parameter. In general, by applying a magnetic field to a fluid flow capable of conduction, the momentum boundary layer is thin. The reason is that during this process resistance forces called Lorentz forces are produced which affect the fluid flow negatively. This force tends to slow down the velocity of the nanofluid past the vertical surface. Figure 3(a) demonstrates that increasing the value of λ_1 decreases the velocity and hence momentum boundary layer thickness decreases. Figures 3(b) shows that the velocity is increased with Gr due to the dominant effects of the buoyancy force in the central region and generates changes in the velocity and high viscous effects across the walls. The velocity is enhanced with the Reynolds number as shown in Figures 4(a). The reason is that as the Reynolds number increases, the inertial force overcomes the flow regarding the viscous forces. High viscous forces are highly resistive to the fluid flows and with strong inertial forces, the flow of the boundary layer decreases.

Figure 4(b) reveals that increasing the values of the magnetic parameter M, increases the temperature of the nanofluid. M generates a resistive force that works contrarily to the flow field and enhances the thermal boundary layer thickness. Figure 5(a) shows that the nanofluid temperature drops when the values of Pr increases, thus the thermal boundary layer decreases for higher quantities of Pr which shows that the effective cooling for nanofluid is achieved quickly. Given the relatively small size of the motion layer the influence of a high Prandtl number is even clearer. Figure 5(b) shows that the enhancement in temperature of the fluid is observed with the increasing values of Nb which results in decrease in the friction of the free surface of nanoparticles. Figure 6(a) shows that the temperature of nanofluid decreases as the Nt values increase. Thermophoresis is a phenomenon of the diffusion of particles because of a temperature gradient effect. The force that transfers nanoparticles to the ambient fluid due to the temperature gradient is called thermophoretic force. Increased thermophoretic force results in a wider transfer of nanoparticles to the fluid layer. The radiation parameter Rd is used to give extra heat to the temperature of the nanoparticles due to an increase in the temperature of the nanofluid as shown in Figure 6(b). The analysis of thermal radiation is of considerable importance in the cooling of the cylinder. The thin film parameter β_1 has a special role in the temperature distribution. The temperature of the thermal boundary surface is high and small along with the transverse distance. The temperature is decelerated by the film thickness parameter for larger quantities, as shown in Figure 7(a). The transfer of heat is improved by thinning the nanofluid. In the present case, however, it is depreciating. The reason for this is that, with the thickness of the fluid film, the mass of the fluid is greater, which exhausts the temperature. As a result, heat penetrates the fluid and the environment is cooling down.

Figure 7(b) and 8(a) portray the influence of the activation energy parameter E and the binary chemical reaction parameter γ_1 on the concentration profile and shows that it is incremented with larger values of E while it is decelerated with enlarging values of γ_1 respectively. The Schmidt number Sc is related to the mass diffusions and therefore increases the mass diffusivity values leading to lessen down the nanoparticle's concentration due to the less mass diffusion transportation as observed in Figure 8(b).

Generally, there is a slight increase in entropy generation with an increase in the magnetic field parameter. The reason is that the magnetic parameter does not have too much influence on the entropy generation, so a large variation in M results in a small variation in entropy as seen in Figure 9(a). It is observed in the Figure 9(b) that the entropy generation increases with the increase in Brinkmann parameter Br. Physically, this is of real significance since $Br(=\Pr Ec)$ is an irreversibility coefficient of fluid friction. The Prandtl number is described as the ratio of thermal to momentum diffusivity, whereas the Eckert number is described as the conversion of kinetic energy into heat through viscous dissipation in the channel/tube. Due to the increase in viscous dissipation, the entropy generation is increased. Figure 10 shows that, as the thermal radiation parameter increases, the rate of entropy generation in the flow is intensified. This is due to an increase in the emission through Rd.

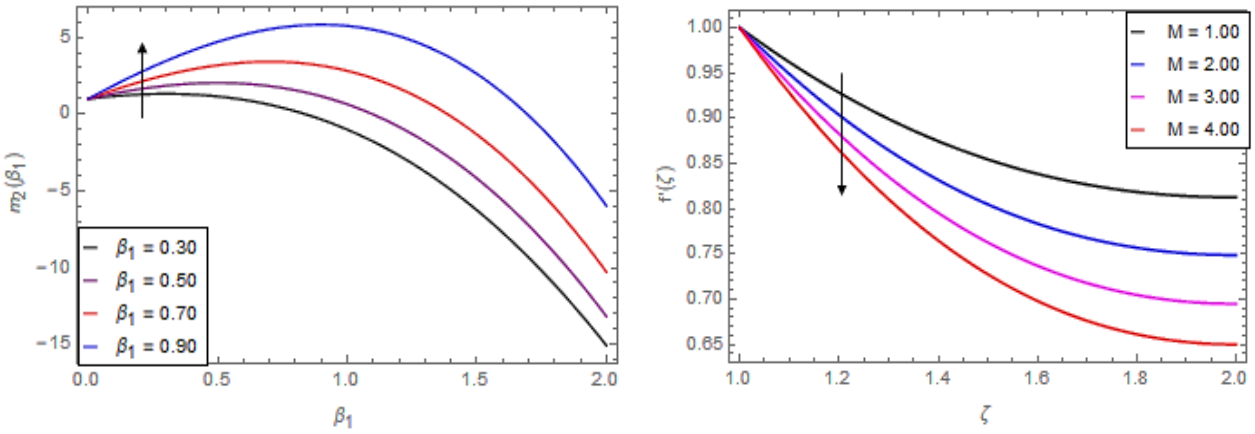

(a) (b)

Fig. 2. (a) Effect of β_1 on $m_2(\beta_1)$ (b) Effect of M on $f'(\zeta)$

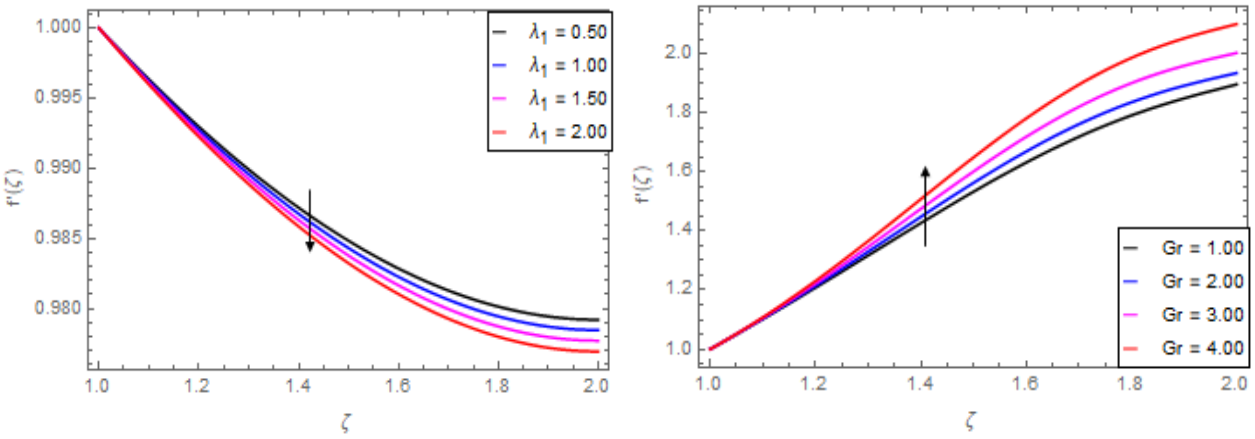

(a) (b)

Fig. 3. (a) Effect of λ_1 on $f'(\zeta)$ (b)) Effect of Gr on $f'(\zeta)$

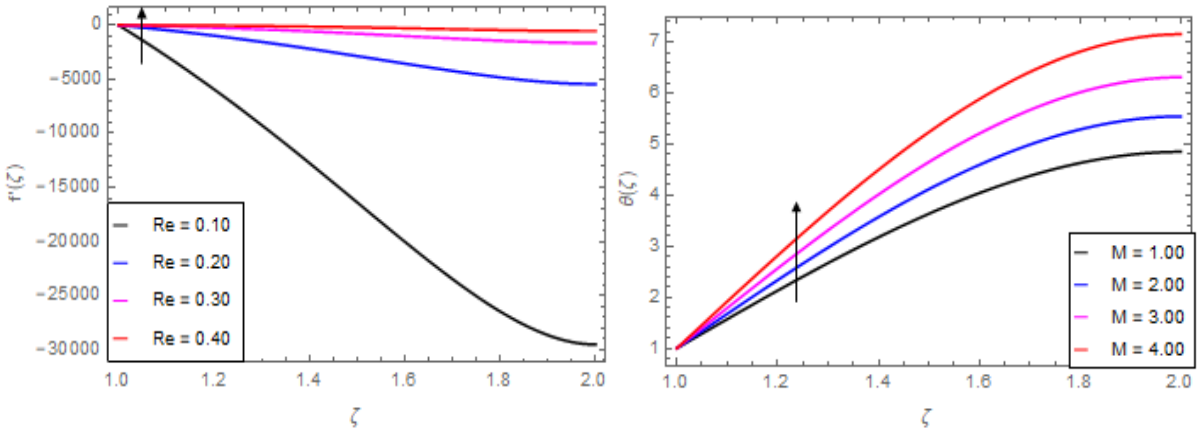

(a) (b)

Fig. 4. (a) Effect of Re on $f'(\zeta)$ (b) Effect of M on $\theta(\zeta)$

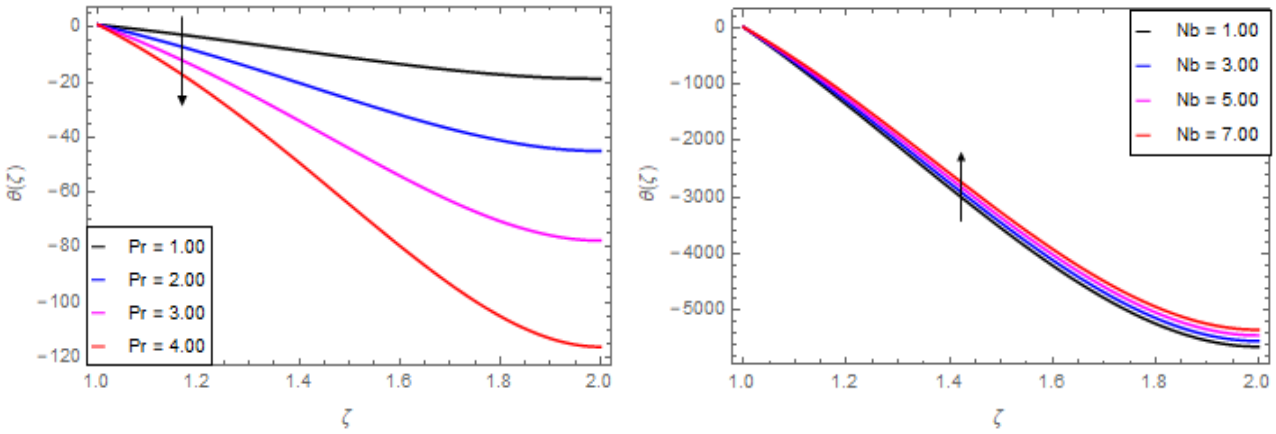

(a) (b)

Fig. 5. (a) Effect of Pr on $\theta(\zeta)$ (b) Effect of Nb on $\theta(\zeta)$

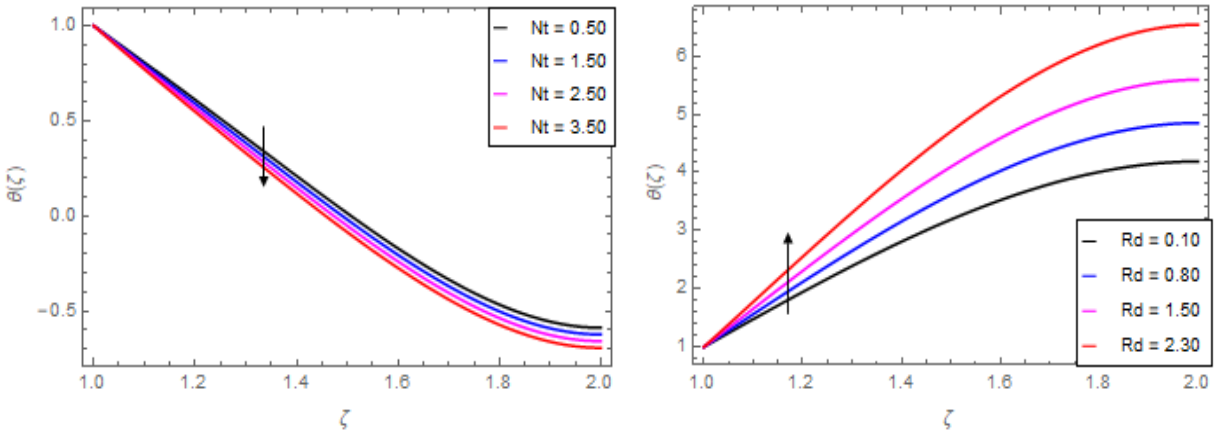

(a) (b)

Fig. 6. (a) Effect of Nt on $\theta(\zeta)$ (b) Effect of Rd on $\theta(\zeta)$

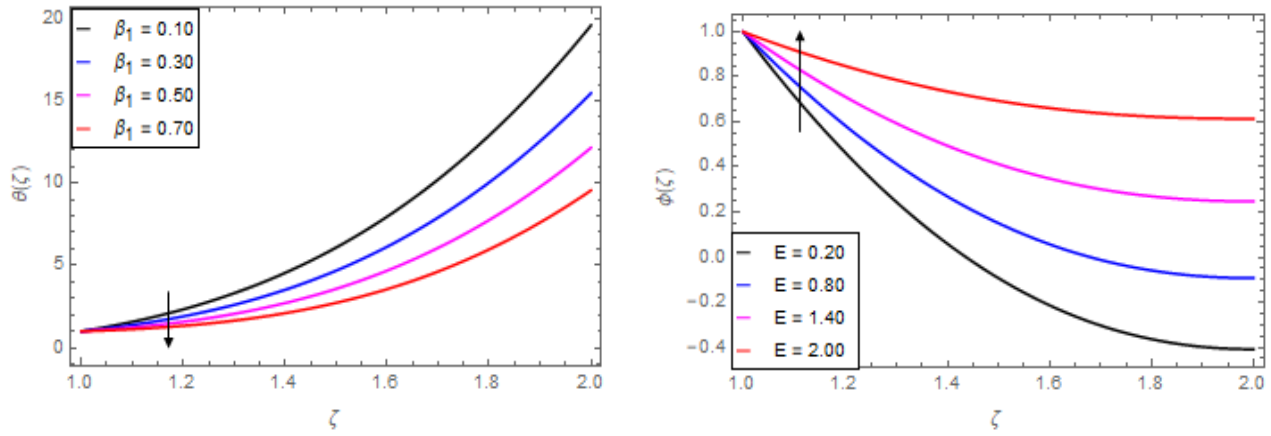

(a) (b)

Fig. 6. (a) Effect of β_1 on $\theta(\zeta)$ (b) Effect of E on $\phi(\zeta)$

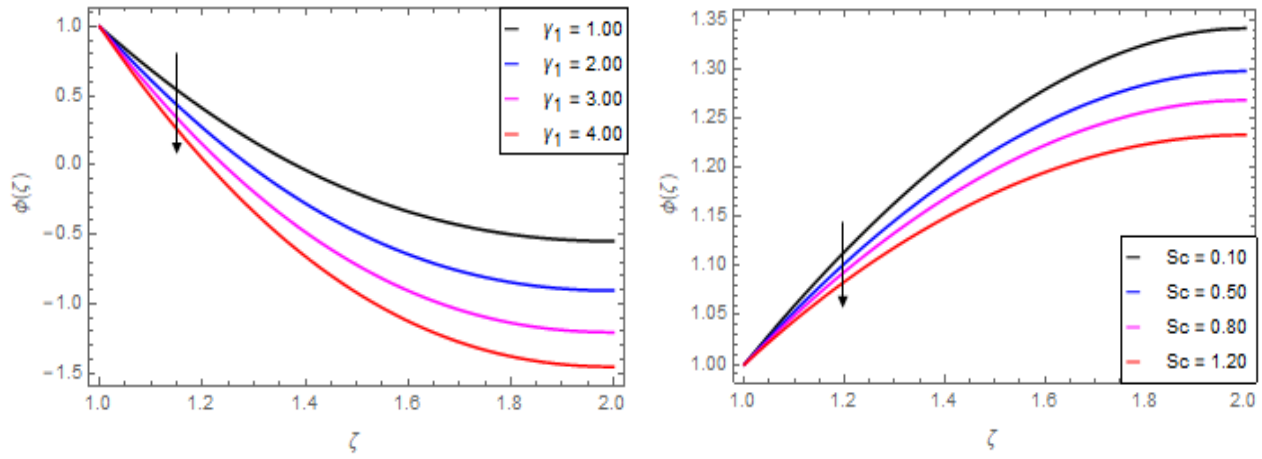

(a) (b)

Fig. 7. (a) Effect of γ_1 on $\phi(\zeta)$ (b) Effect of Sc on $\phi(\zeta)$

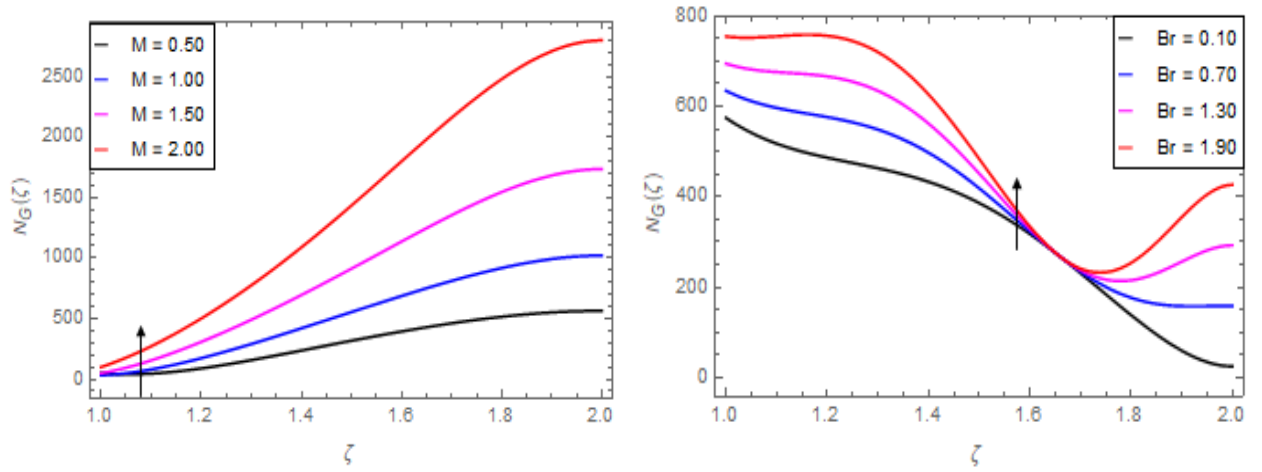

(a) (b)

Fig. 8. (a) Effect of M on $N_G(\zeta)$ (b) Effect of Br on $N_G(\zeta)$

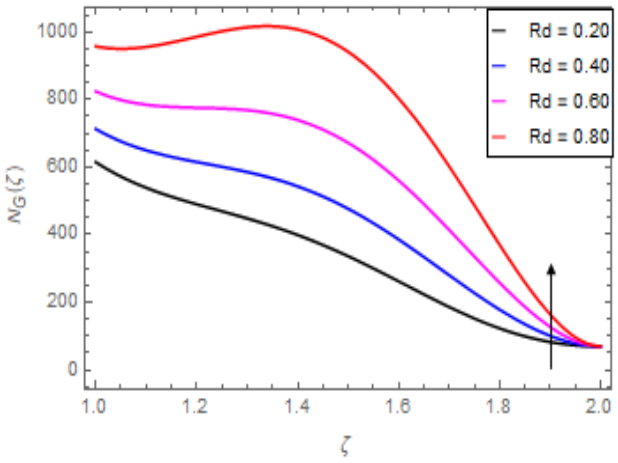

Fig. 10. Effect of Rd on $N_G(\zeta)$

6.1 Comparison of the present work with published work

The present work is compared with the published work [27] for various values of $\Pr$ parameter which shows the close agreement as shown in Table I. Convergence of series solutions for different order of approximations shown in Table II.

Table I
Comparison of $-\theta'(1)$ for various values of $\Pr$ the present research with published paper

Pr	Hayat et al. [27]	Present work
1.0	-1.0000	-1.0000
	0.0	0.0
	0.5832	0.5832
	1.0000	1.0000
	1.3332	1.3334
10	-10.0000	-10.0000
	0.0	0.0
	2.3080	2.3076
	3.7207	3.7210
	4.7969	4.7971
0.9	1.2507	1.2507
0.8	1.1662	1.1659
0.7	1.0791	1.0793

Table II
Convergence of series solutions for different order of approximations

Oder of Approximation	$-f''(1)$	$-\theta'(1)$	$-\phi'(1)$
1	0.7231	0.6013	0.6033
10	0.6232	0.5599	0.6000
20	0.5331	0.5570	0.5891
21	0.5131	0.5569	0.5891
25	0.5100	0.5569	0.5891
30	0.5002	0.5569	0.5891
40	0.4991	0.5569	0.5891

7. Conclusions

The viscoelastic nano-liquid film sprayed on the stretch cylinder is evaluated for mass and heat transfer flow. Thermodynamics and spray phenomena are mathematically modelled and then analysed using a HAM solution with profiles such as spray rate, velocity, heat and mass transfer. Reynolds number Re and film thickness parameter β_1 have important roles in the spraying phenomena on a stretching cylinder. Other applications in the current studies show that the stretching material is sprayed with Newtonian or non-Newtonian nanofluids for coolant, film and paint protection. Current research offers an effective exchange of innovative scientific and engineering ideas and the dissemination of recent, original and significant research and development observations. The spray rate does not increase linearly with the thickness of the film. Details of the results obtained are discussed in the discussion section.

Acknowledgement
The authors appreciate the financial support allotted by King Mongkut's University of Technology Thonburi through the "KMUTT 55th Anniversary Commemorative Fund". The first author is supported by the Petchra Pra Jom Klao Doctoral Scholarship Academic for PhD studies at KMUTT. The research is funded by Petchra Pra Jom Klao Doctoral Scholarship for Ph.D. program of King Mongkut's University of Technology Thonburi (KMUTT) (Grant No. 13/2562). Moreover, this research project is supported by Thailand Science Research and Innovation (TSRI) Basic Research Fund: Fiscal year 2021 under project number 64A306000005.

References

[1] Albano, P. G., Borghi, C.A., Cristofolini, A., Fabbri, M.; Kishimoto, Y., et al. Industrial applications of magnetohydrodynamics at the University of Bologna. *Energy Convers. Manag*. 43, 353-63 (2002).
[2] Han, S., Zheng, L., Li, C. and Zhang, X., 2014. Coupled flow and heat transfer in viscoelastic fluid with Cattaneo–Christov heat flux model. *Applied Mathematics Letters*, *38*, pp.87-93.
[3] Mrokowska, M.M. and Krztoń-Maziopa, A., 2019. Viscoelastic and shear-thinning effects of aqueous exopolymer solution on disk and sphere settling. *Scientific reports*, *9*(1), pp.1-13.
[4] Li, J., Zheng, L. and Liu, L., 2016. MHD viscoelastic flow and heat transfer over a vertical stretching sheet with Cattaneo-Christov heat flux effects. *Journal of Molecular Liquids*, *221*, pp.19-25.
[5] Kumar, A., JV, R.R., Sugunamma, V. and Sandeep, N., 2018. Impact of cross diffusion on MHD viscoelastic fluid flow past a melting surface with exponential heat source. *Multidiscipline Modeling in Materials and Structures*.
[6] Kumar, B.R. and Sivaraj, R., 2013. Heat and mass transfer in MHD viscoelastic fluid flow over a vertical cone and flat plate with variable viscosity. *International Journal of Heat and Mass Transfer*, *56*(1-2), pp.370-379.
[7] Khan, N.S., Shah, Z., Islam, S., Khan, I., Alkanhal, T.A. & Tlili, I. Entropy generation in MHD mixed convection non-Newtonian second grade nanoliquid thin film flow through a porous medium with chemical reaction and stratification. *Entropy* 21, 139 (2019).
[8] Rashidi, M.M., Ali, M., Freidoonimehr, N., Rostami, B. and Hossain, M.A., 2014. Mixed convective heat transfer for MHD viscoelastic fluid flow over a porous wedge with thermal radiation. *Advances in Mechanical Engineering*, *6*, p.735939.
[9] Choi, S.U. & Eastman, J.A. Enhancing thermal conductivity of fluids with nanoparticles. *Argonne National Lab., IL (United States)* (1995).
[10] Buongiorno, J. Convective transport in nanofluids. *J. Heat Transf.* 128, 240–250. (2006).
[11] Ellahi, R., Zeeshan, A., Hussain, F. & Abbas, T. Thermally charged MHD bi-phase flow coatings with non-Newtonian nanofluid and hafnium particles along slippery walls. *Coatings* 9, 300 (2019).
[12] Ellahi, R., Zeeshan, A., Hussain, F. & Abbas, T. Study of shiny film coating on multi-fluid flows of a rotating disk suspended with nano-sized silver and gold particles: A comparative analysis. *Coatings*, 8, 422 (2018).
[13] Khan, N.S., Gul, T., Islam, S., Khan, I., Alqahtani, A.M. & Alshomrani, A.S. Magnetohydrodynamic nanoliquid thin film sprayed on a stretching cylinder with heat transfer. *Appl. Sci*. *7*, 271 (2017).
[14] Palwasha, Z., Islam, S., Khan N.S. & Ayaz H. Non-Newtonian nanoliquids thin-film flow through a porous medium with magnetotactic microorganisms. *Appl. Nanosci*. 8, 1523-44 (2018).

[15] Hartig, K. & Krisko, A.J. Inventors Cardinal CG Co, assignee. Thin film coating having transparent base layer. *United States patent US*, 919, 133 (2005).
[16] S. Arrhenius, "Über die Dissociationswärme und den Einfluss der Temperatur auf den Dissociationsgrad der Elektrolyte" *Z. Phys. Chem.* 4(1), 96-116 (1889).
[17] A. R. Bestman. Natural convection boundary layer with suction and mass transfer in a porous medium. *Int. J. Energy Res.* 14(4), 389-396 (1990).
[18] Kumar, K. G., Baslem, A., Prasannakumara, B. C., Majdoubi, J., Rahimi-Gorji, M., & Nadeem, S. Significance of Arrhenius activation energy in flow and heat transfer of tangent hyperbolic fluid with zero mass flux condition. *Microsyst. Technol.* 1-10 (2020).
[19] Alghamdi, M. Significance of Arrhenius activation energy and binary chemical reaction in mixed convection flow of nanofluid due to a rotating disk. *Coatings* 10, 86 (2020).
[20] Ramesh, G. K. Analysis of active and passive control of nanoparticles in viscoelastic nanomaterial inspired by activation energy and chemical reaction. *Physica A.* 550, 123964 (2020).
[21] Khan, N.S., Kumam, P. & Thounthong, P. Second law analysis with effects of Arrhenius activation energy and binary chemical reaction on nanofluid flow. *Sci. Rep*., 10, 1-6 (2020).
[22] Abdelmalek, Z., Mahanthesh, B., Basir, M.F., Imtiaz, M., Mackolil, J. et al. Mixed radiated magneto Casson fluid flow with Arrhenius activation energy and Newtonian heating effects: Flow and sensitivity analysis. *Alex. Eng. J*. (2020).
[23] Wang, C.Y. Fluid flow due to a stretching cylinder, *Phys. Fluids* 31, 466-468 (1988).
[24] Bachok, N. & Ishak, A. Flow and heat transfer over a stretching cylinder with prescribed surface heat flux. *Malaysian J. Math. Sci*. 4, 159-169 (2010).
[25] Chuhan, D.S., Rastogi, P. & Agrawal, R. Magnetohydrodynamic flow and heat transfer in a porous medium along a stretching cylinder with radiation: homotopy analysis method. *Afrika Mat*. 25, 115-134 (2014).
[26] Hayat, T., Waqas, M., Shehzad, S.A. & Alsaedi, A. Mixed convection flow of viscoelastic nanofluid by a cylinder with variable thermal conductivity and heat source/sink. *Int. J. Numer. Method H.* (2016).
[27] Wang, C.Y. Liquid film sprayed on a stretching cylinder. *Chem. Eng. Commun*. *193*, 869-878 (2006).
[28] Liao, S.J. The proposed homotopy analysis method for the solution of nonlinear problems. Ph.D. Thesis, *Shanghai Jiao Tong University, Shanghai, China* (1992).
[29] Liao, S.J. An Explicit, Totally analytic approximate solution for Blasius viscous flow problems. *Int. J. Non-Linear Mech.* 34, 759–778 (1999).
[30] Liao S. Beyond perturbation: Introduction to the homotopy analysis method. *CRC press; Boca Raton, FL, USA*. (2003).
[31] Rashidi, M.M., Siddiqui, A.M. & Asadi, M. Application of homotopy analysis method to the unsteady squeezing flow of a second-grade fluid between circular plates. *Math. Probl. Eng*. (2010).
[32] Shah, Z., Gul, T., Khan, A.M. Ali, I. & Islam, S. Effects of hall current on steady three-dimensional non-Newtonian nanofluid in a rotating frame with Brownian motion and thermophoresis effects. *J. Eng. Technol*. 6, 280–296 (2017).